Hindawi
Advances in Materials Science and Engineering
Volume 2022, Article ID 3982415, 8 pages
https://doi.org/10.1155/2022/3982415

Research Article

Fatigue Failure Analysis of a Gear in Automobile Engine Coolant Pump

Krishnakumar Krishnasamy,[1] **D. Subbulekshmi**,[2] **T. Deepa**,[2] **B. M Gnanasekaran**,[3] **T. Maridurai**,[4] **M. Sriram**,[5] **Srinivasan Suresh Kumar**,[6] **and Mebratu Markos**[7]

[1]*Sr.Manager-Product Development (Engineering), TIDC INDIA, Chennai-600 053, Tamil Nadu, India*
[2]*School of Electrical Engineering, Vellore Institute of Technology, Chennai-600127, Tamil Nadu, India*
[3]*Department of Mechanical Engineering, Fatima Michael College of Engineering and Technology, Madurai – 625020, Tamil Nadu, India*
[4]*Department of Mechanical Engineering, Saveetha School of Engineering, SIMATS, Chennai 602105, Tamil Nadu, India*
[5]*Department of Computer Science Engineering, Bharath Institute of Higher Education and Research, Chennai 600073, Tamil Nadu, India*
[6]*Department of Mechanical Engineering, Panimalar Polytechnic College, Chennai - 600029, Tamilnadu, India*
[7]*Department of Mechanical Engineering, College of Engineering, Wolaita Sodo University, Ethiopia*

Correspondence should be addressed to Krishnakumar Krishnasamy; krishnaksp07@gmail.com

Received 15 December 2021; Accepted 1 February 2022; Published 27 March 2022

Academic Editor: P Ganeshan

Gear is a reliable part of power transmission. This article presents a metallurgical failure analysis of a failed gear used in automobile engine coolant pumps. In gear, the soft microstructure of pearlite and ferrite is witnessed in metallographic analysis. Significant wear is perceived in gear teeth, and significant deformation is observed in the keyway. The crack initiated from the corner radius of the keyway and propagated towards to the root of the teeth, which is evidence of the failure due to fatigue. Recommendations are given to improve the fatigue strength of gear.

1. Introduction

Gear is a reliable power transmission element and is extensively used in automobile and industrial drive applications. There is no intermediate link or connector on the gear, and it transmits the motion by direct contact. Gear is the most frequently failed member in applications. Common failures in gear are pitting, spalling, wear, and fatigue. The failed reducing gear used in the petrochemical industry is carburized, quenched, and tempered. The microstructure of the case is tempered high carbon martensite, and the core is low carbon martensite. The fatigue failure occurred from poorly designed drill holes, which are used for handling large-sized gear [1]. Helical gear in a power generation plant has failed due to fatigue fracture. During microanalysis, inclusions are identified in material with iron oxide surrounded by (FeMo) 3C carbide. The inclusions [2] are formed during the gear blank casting process. The planetary gear failed due to tooth pitting [3] and cracking. The pinion gear crack is originated from small cavities caused by micropitting. In such conditions, the surface is overstressed, and induced plastic deformation by the ridge formation [4] occurs at the bottom of the root fillet. The pinion was loaded heavily near the thrust disc and stress increased in the pinion teeth, which resulted in plastic deformation [5] of the teeth. The author suggested redesigning the pinion assembly to sustain the working load. The failed gear was made up of 20CrNiMo, and surface pitting [6] appeared near the pitch line of the teeth. The gear of the helicopter is rigorously destroyed by spalling [7]. Fractographic analysis confirms the crack originated at the root of the gear. On the other hand, inadequate lubrication, improper mounting, poor

maintenance, unsuitable material selection, and improper heat treatment of drive components result in failure [8–13]. Prior to starting the failure analysis, a literature review is done to realize the various mechanisms of the gear and drive components. Case studies are very useful to understand the causes of drive component failure and the methodology of failure analysis. Most research papers are focussed on failure analysis of helical gear, planetary gear, chains, and drive components used in different applications [14–16]. Limited papers are available on the fatigue failure analysis of gears in automobile applications. Therefore, the motivation behind this investigation is to direct metallurgical examination on a failed engine coolant pump gear and recommend to enhancing the fatigue strength.

2. Materials and Methods

The engine coolant pump gear may fail in function. Analysis of failure detection is conducted using the methods of visual examination, chemical analysis, hardness analysis, scanning electron microscopy (SEM) analysis, and metallographic analysis. The failed gear is made up of EN353 material grade. Experimental tests (ultimate tensile and hardness) are conducted on cylindrical test specimens for performance comparison [33–36]. Test methods are described as follows, and results and discussion are provided. This case study describes the failure analysis of gear that has failed in service [17, 18]. It is reported that the gear is part of the engine coolant pump assembly. Basically, the engine coolant pump consists of the housing, mechanical seal, gear, o-ring, impeller, and integral shaft bearing as shown in Figure 1(a). Integral shaft bearing and mechanical seal are press-fitted with housing. Gear with key is press-fitted at one end of the shaft, and the impeller is press-fitted at the other end of the shaft [25–28].

2.1. Visual Examination. Failed gear has a keyway in the inner diameter and a gear tooth profile in the outer diameter, as shown in Figure 1(c). The gear had failed in a longitudinal mode lengthwise, as shown in Figure 1(b). The longitudinal mode crack occurs up to 65% of the length, and significant wear is perceived in the gear profile [15, 19, 20]. The crack initiated from the corner radius of the keyway and propagated towards the root diameter of the gear.

The gear is cut in a cross-sectional view where the longitudinal mode is ended and cross-sectional keyway of the remaining portion, is shown in Figure 2(a). A close-up view of the remaining part, as shown in Figure 2(b), confirms the enlarged keyway portion. The deep deformation of the keyway is due to the heavy load during application.

2.2. Chemical Analysis. The chemical composition of the failed gear is analysed by optical emission spectroscopy. Table 1 shows the EN353 specifications with the chemical composition of the failed gear. This type of material is typically case-hardened and used in drive components such as bearings, shafts, and spinning tools. The presence of nickel 1.00–1.50% increases the toughness, while molybdenum 0.08–0.15% and chromium 0.75–1.25% contribute to increasing the case harden surface, resulting in an improvement in wear resistance [21–24].

2.3. Hardness Measurement. Hardness measurements are carried out on metallographically polished samples from an area away from the fracture area. A rockwell hardness tester is used to measure the hardness from the cross section of the keyway radius and to the root of the gear radius. The average hardness value is 89 HRB. The hardness indicates the part is not heat-treated. It is in soft condition.

2.4. Scanning Electron Microscopy Analysis. The entirely fractured surfaces are washed by using acetone and diluted HCL. The crack initiated from the keyway edge and propagated towards the root diameter of the gear tooth. The low magnification SEM image (Figure 3(a)) indicates that the top area is the tooth surface and bottom area is the keyway surface. In between the tooth and keyway surface, the crack origin, fatigue propagation zone, and overload zone are presented. Fatigue propagated zone stand up before the overload zone. Figure 3(b) shows the increased magnification SEM view of the fracture surface at the crack origin.

The high magnification shows the fracture origin exposed fatigue striations (beach marks) in Figure 4(a), and the beach marks are concentric rings in a fatigue region which resembles wave marks on a beach. The crack progression is caused by changes in working load and environment. The overload high magnification SEM view in Figure 4(b) revealed a dimpled feature. The dimpled features occurred due to the creation and coalescence of microvoids sideways to the fracture mode. This confirms the ductile overload fracture.

2.5. Metallography. In optical microscopic observation, a minor crack is observed at the corner radius of the keyway shown in Figure 5(a). A considerable grain deformation was also observed in the keyway radius. The fatigue crack initiated from the keyway edge radius and propagated towards the root of the teeth. In the microstructure of the core, soft pearlite and ferrite are perceived, as shown in Figure 5(b). It is confirmed that gear is not heat-treated [29–32].

3. Results and Discussion

The cylindrical test specimens are prepared using a turning center and the dimensions of the specimen are as per the ASTM E8 standard. The specimens are made up of EN353 material. Four specimens are prepared as shown in Figure 6(a). Specimens 1 and 2 are not heat-treated (soft) condition, and specimens 3 and 4 are heat-treated by the case hardening process. Specimens 1 and 3 have undergone hardness testing. Specimens 2 and 4 have been submitted for tensile testing.

3.1. Hardness Test of Specimen. Specimens 3 and 4 are case-hardened by using a mesh belt furnace. The case hardening process cost is approximately 5% of the gear cost. The

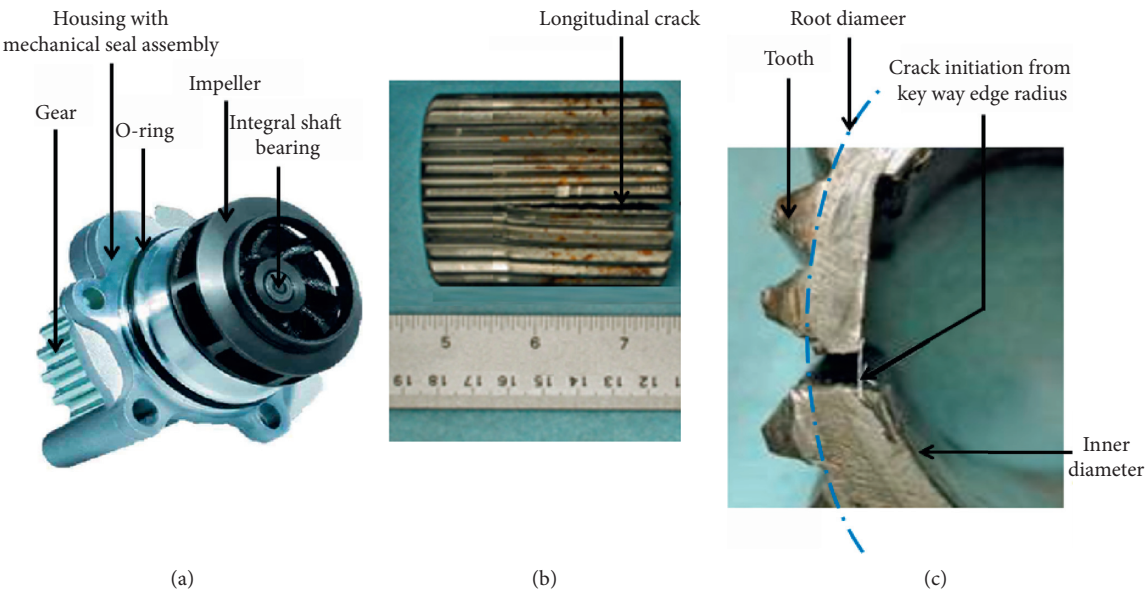

Figure 1: (a) Parts of an engine coolant pump, (b) Crack geometry of the failed gear, (c) Crack initiation.

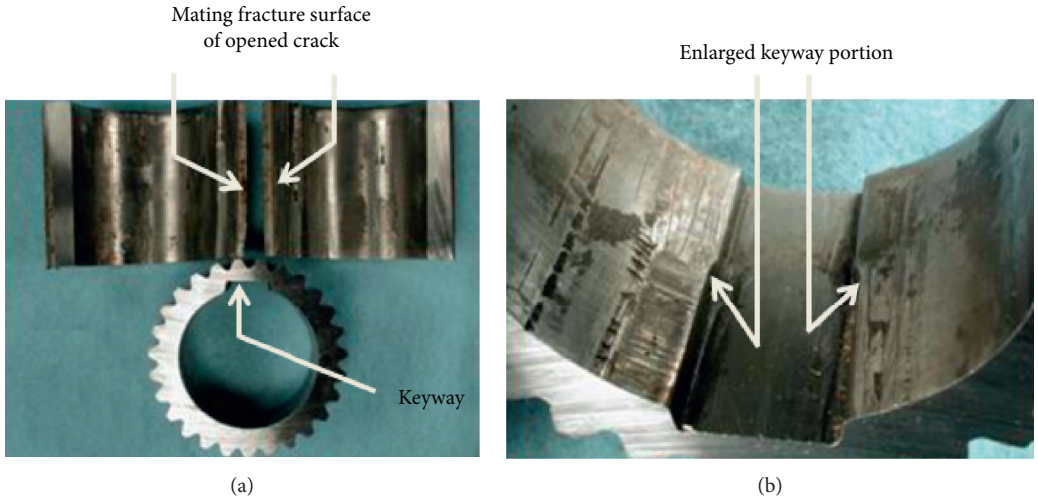

Figure 2: (a) Overview of longitudinal mode crack surface and the cross-sectional view of keyway at the nonfailed portion. (b) Enlarged keyway portion of gear.

Table 1: Failed gear chemical composition compared to the related grade (% wt.).

Sample	C%	Mn%	Si%	S%	P%	Cr%	Mo%	Ni%
Gear #1	0.16	0.99	0.26	0.026	0.005	1.09	0.12	1.15
EN353	0.10–0.20	0.50–1.00	0.10–0.35	0.040 max	0.040 max	0.75–1.25	0.08–0.15	1.00–1.50

microstructure of the specimen is analysed using a Leica DMC2900 microscope. Microstructure is carried out on a metallographically polished specimen 3. Fine-tempered martensite microstructure in the case surface is presented in Figure 7(a), and low carbon martensite microstructure in the core is revealed in Figure 7(b). Readings of hardness are taken in a 15 N : 15 kgf superficial rock well. The surface hardness of specimen 3 is 48.5 HR15 N. The case depth of the outer diameter is 0.35 mm. Core hardness is found to be 415 HV @ 0.20 kgs, as shown in the microhardness traverse survey graph in Figure 7(c). The hardness of the soft specimen 1 is in the range of 180 to 190 HV at 0.20 kgs. (88 to 90 HRB). Rockwell B is shown in the microhardness traverse survey graph in Figure 7(c).

3.2. Tensile Strength Test. The ultimate tensile stress (UTS) of EN353 specimens is tested by using the 1000-ton capacity universal testing machine (UTM). Universal fixtures are designed according to the specimen. In UTM, the upper

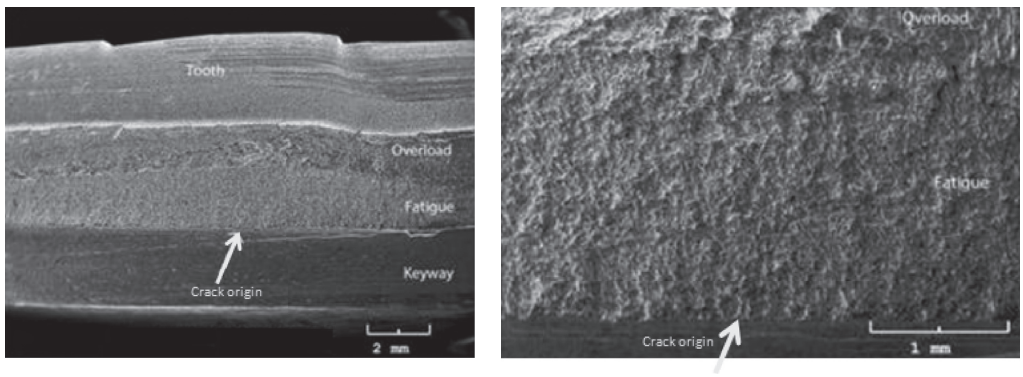

(a) (b)

Figure 3: (a) SEM image of the fractured surface (magnification: 10x). (b) SEM micrograph showing the crack origin, fatigue zone, and overload zone of the fracture surface (magnification: 40x).

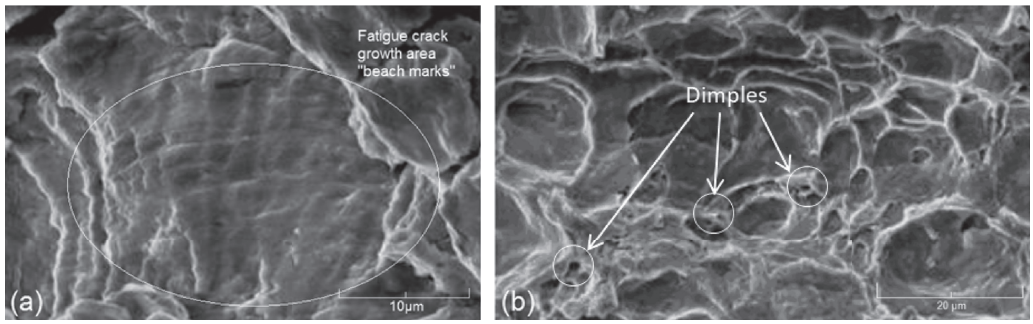

Figure 4: (a) SEM micrograph showing the fatigue (magnification: 4000x). (b) SEM micrograph showing the dimpled surface feature (magnification: 2000x).

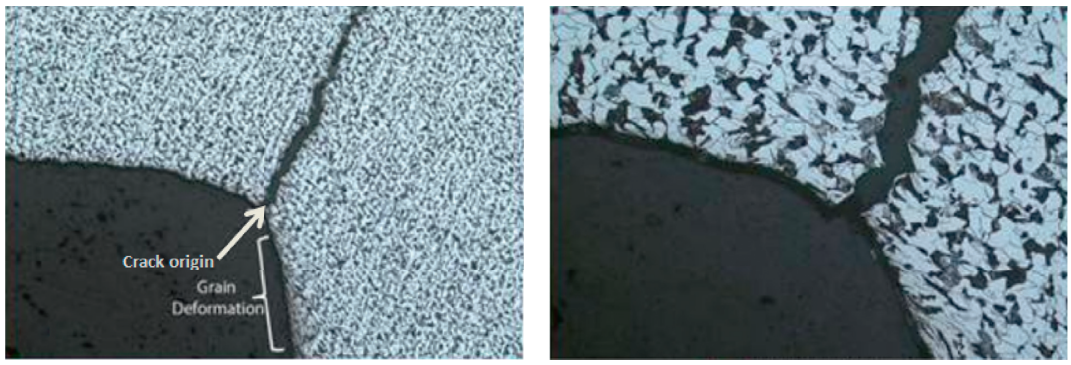

(a) (b)

Figure 5: (a) Optical microscopic view showing the crack origin at the corner radius of keyway (magnification: 50x). (b) Microstructure shows the soft pearlite and ferrite in the core (magnification: 200x).

cross head is the fixed end and the lower is the movable end. The specimen is fixed between two ends as shown in Figure 6(b).

Soft specimen 2 and case-hardened specimen 4 are tested. The stress-strain curve and load-displacement curve of the soft specimen are shown in Figure 8(a) and Figure 8(b), respectively. The stress-strain curve and load-displacement curve of the hardened specimen are shown in Figure 9(a) and Figure 9(b), respectively. The ultimate tensile stress (UTS) of soft specimen 2 is 940 Mpa, whereas hardened specimen 4 is 1495 MPa. Hence, 59% of the ultimate tensile stress (UTS) is higher in hardened specimen 4.

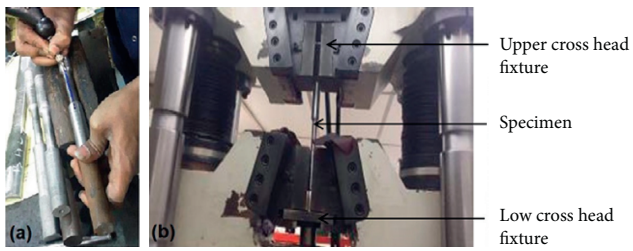

Figure 6: (a) Sample specimens. (b) Tensile test (UTM) machine setup.

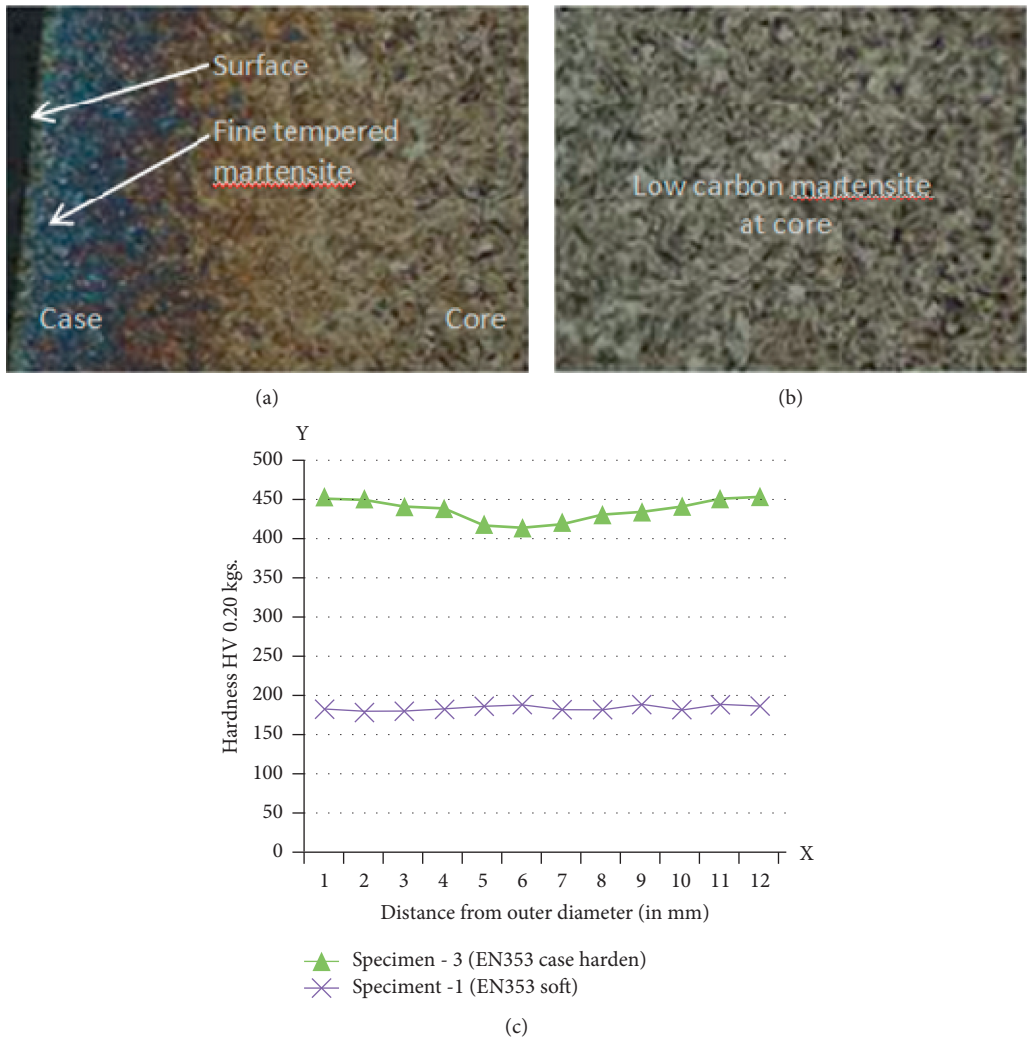

Figure 7: (a) Specimen 3 microstructure shows the finely tempered martensite in the case. (b) Specimen 3 microstructure reveals low carbon martensite in the core. (c) Microhardness traverse survey graph.

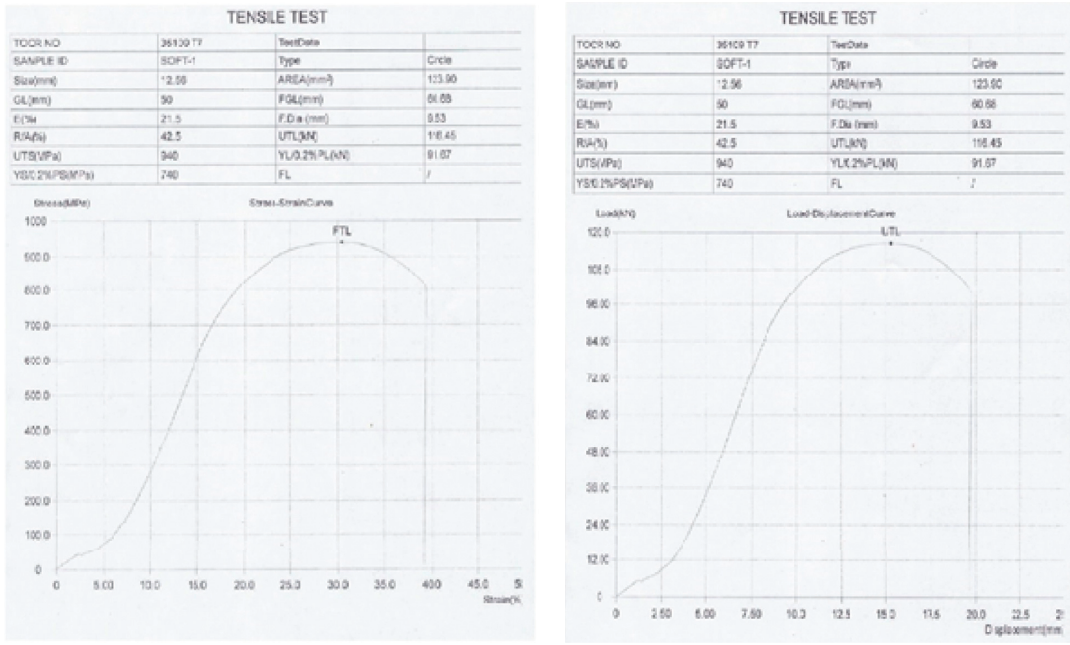

(a) (b)

Figure 8: (a) Stress-strain curve of soft specimen 2. (b) Load-displacement curve of soft specimen 2.

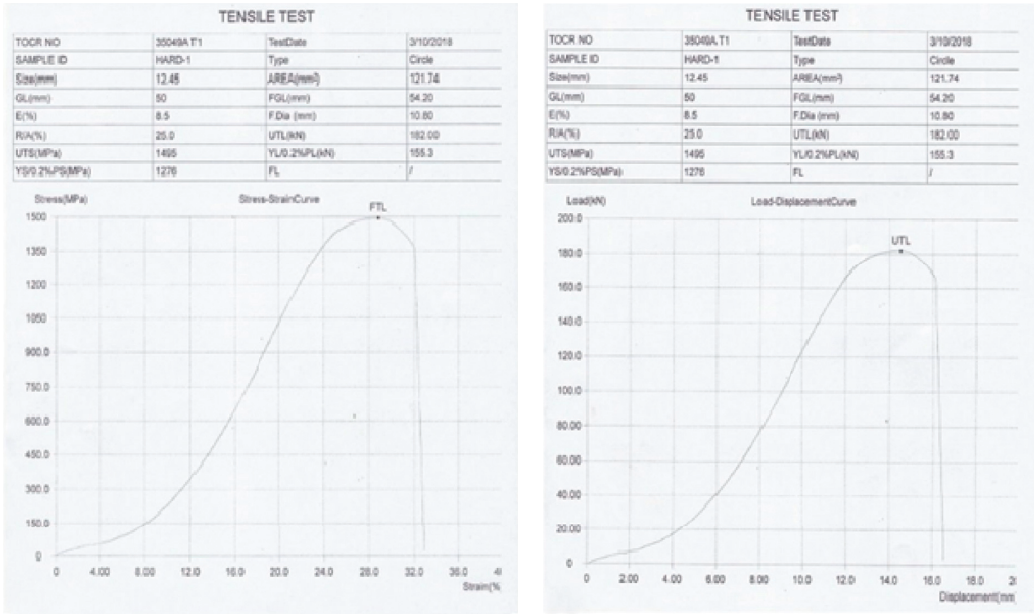

(a) (b)

Figure 9: (a) Stress-strain curve of hardened specimen 4, (b) Load-displacement curve of hardened specimen 4.

4. Conclusion

The crack initiated from the corner radius of the keyway and propagated towards the root of the gear, which confirmed the failure was due to fatigue. Significant wear is observed in gear teeth, and significant deformation is observed in the keyway. A soft microstructure of pearlite and ferrite is observed in metallographic analysis, and an average hardness of 89 HRB confirms that the gear is not heat-treated.

The following measures can be taken to avoid the failure of the gear:

(1) Keyway edge radius to be increased to reduce stress concentrations in the area of fatigue crack origin.

(2) Based on tensile test validation in samples, by the case hardening process, 59% of tensile strength was improved.

(3) The case hardening process followed by quenching and tempering could confidently increase the wear resistance and the fatigue strength of the gear.

Data Availability

The data used to support the findings of this study are included within the article. Further data or information are available from the corresponding author upon request.

Conflicts of Interest

The authors declare that there are no conflicts of interest regarding the publication of this article.

References

[1] S. Griza, A. P. Santos, T. F. Azevedo, C. E. F. Kwietniewski, A. Reguly, and T. R. Strohaecker, "Failure analysis of a petrochemical plant reducing gear," *Engineering Failure Analysis*, vol. 29, pp. 56–61, 2013.

[2] F. Chaari, T. Fakhfakh, and M. Haddar, "Dynamic analysis of a planetary gear failure caused by tooth pitting and cracking," *Journal of Failure Analysis and Prevention*, vol. 6, no. 2, pp. 73–78, 2006.

[3] M. Boniardi, F. D'Errico, and C. Tagliabue, "Influence of carburizing and nitriding on failure of gears - a case study," *Engineering Failure Analysis*, vol. 13, no. 3, pp. 312–339, 2006.

[4] Q. Wang, Y. Zhu, Z. Zhang, C. Fu, C. Dong, and H. Su, "Partial load: a key factor resulting in the failure of gear in the wind turbine gearbox," *Journal of Failure Analysis and Prevention*, vol. 16, no. 1, pp. 109–122, 2016.

[5] S. K. Bhaumik, M. Sujata, M. S. Kumar, M. A. Venkataswamy, and M. A. Parameswara, "Failure of an intermediate gearbox of a helicopter," *Engineering Failure Analysis*, vol. 14, no. 1, pp. 85–100, 2007.

[6] K. Raja, V. S. Chandra Sekar, V. Vignesh Kumar, T. Ramkumar, and P. Ganeshan, "Microstructure characterization and performance evaluation on AA7075 metal matrix composites using RSM technique," *Arabian Journal for Science and Engineering*, vol. 45, no. 11, pp. 9481–9495, 2020.

[7] K. Krishnasamy, "Investigation on metallurgy and material strength enhancement of 20MnCr5 forged link chain in cement mill," *World Review of Science, Technology and Sustainable Development*, vol. 17, pp. 197–210, 2021.

[8] V. V. Kumar, K. Raja, V. S. Chandra Sekar, and T. Ramkumar, "Thrust force evaluation and microstructure characterization of hybrid composites (Al7075/B4C/BN) processed by conventional casting technique," *Journal of the Brazilian Society of Mechanical Sciences and Engineering*, vol. 41, pp. 214–228, 2019.

[9] K. Krishnasamy, "Arockia selvakumar arockia doss, "metallurgical failure analysis and improved core hardness to enhance crushing strength," *Wear Resistance and Fatigue Strength of Chain Bush"*, vol. 20, pp. 967–975, 2020.

[10] M. Rajeshwaran, P. Ganeshan, and K. Raja, "Optimization and biodiesel production from prosopis julifera oil with high free fatty acids," *Journal of Applied Fluid Mechanics*, vol. 11, no. 1, pp. 257–270, 2018.

[11] K. Krishnakumar and A. Arockia Selvakumar, "Enhancement of fatigue strength on SAE 1541 steel link plate with slip ball burnishing technique," *Defence Science Journal*, vol. 70, no. 4, pp. 454–460, 2020.

[12] N. Sivanandham, A. Rajadurai, S. M. Shariff, J. Senthilselvan, and A. Mahalingam, "Microstructure, mechanical properties and corrosion resistance of laser surface melted EN353 low carbon low alloy steel," *International Journal of Surface Science and Engineering*, vol. 11, no. 2, pp. 118–132, 2017.

[13] M. Balu, K. Lingadurai, P. Shanmugam, K. Raja, N. Bhanu Teja, and V. Vijayan, "Biodiesel production from caulerpa racemosa (macroalgae) oil," *International Journal of Mathematics and Statistics*, vol. 49, no. 4, pp. 616–621, 2020.

[14] V. Kumar, K. Raja, K. Chandrasekaran, and T. Ramkumar, "Effect on the behaviour of dynamic mechanical analysis for hybrid epoxy/BN metal matrix composites prepared by conventional casting method," *Materials Research Express*, vol. 6, p. 6, 2019.

[15] V. Yamunadevi, G. Vijayanand, P. Ganeshan, S. Sowmiya, and K. Raja, "Effect on the behaviour of dynamic mechanical analysis for hybrid epoxy nanocomposite," *Materials Today Proceedings*, vol. 37, 2020.

[16] G. Radhaboy, M. Pugazhvadivu, P. Ganeshan, and K. Raja, "Influence of kinetic parameters on calotropis procera by TGA under pyrolytic conditions," *Energy Sources, Part A: Recovery, Utilization, and Environmental Effects*, 2019.

[17] N. Saravanan, P. Ganeshan, B. Prabu, V. Yamunadevi, B. NagarajaGanesh, and K. Raja, "Physical, chemical, thermal and surface characterization of cellulose fibers derived from vachellia nilotica Ssp. indica tree barks," *Journal of Natural Fibers*, 2021.

[18] K. Raja, B. Prabu, P. Ganeshan, V. S. Chandra Sekar, and B. Nagaraja Ganesh, "Characterization studies of natural cellulosic fibers extracted from shwetark stem," *Journal of Natural Fibers*, vol. 18, no. 11, pp. 1934–1945, 2020.

[19] R. Ramkumar, R. Prabu, V. Yamunadevi, P. Saravanan, and P. Ganeshan, "Wear analysis of woven glass/nanofiller fiber reinforced hybrid composites," *Materials Today Proceedings*, Elsevier, 2020.

[20] P. Sainath, F. Mohammed Ajmal Sheriff, and P. Ganeshan, "Fabrication of hybrid polyester composites in various combinations and evaluate the mechanical properties," *Materials Today Proceedings*, Elsevier, 2020.

[21] V. Yamunadevi, K. Palaniradja, A. Thiagarajan, P. Ganeshan, and K. Raja, "Characterization and dynamic mechanical analysis of woven roven glass fiber/cerium- zirconium oxide epoxy nanocomposite materials," *Mater. Res. Express, IOP*, vol. 6, Article ID 095057, 2019.

[22] N. Saravanan, V. Yamunadevi, V. Mohanavel et al., "Effects of the interfacial bonding behavior on the mechanical properties of E-glass fiber/nanographite reinforced hybrid composites," *Advances in Polymer Technology*, vol. 2021, Article ID 6651896, 9 pages, 2021.

[23] V. Mohanavel, S. Suresh Kumar, J. Vairamuthu, P. Ganeshan, and B. NagarajaGanesh, "Influence of stacking sequence and fiber content on the mechanical properties of natural and synthetic fibers reinforced penta-layered hybrid composites," *Journal of Natural Fibers*, Taylor & Francis, 2021.

[24] K. Yoganandam, K. Raja, P. Ganeshan, and V. Mohanavel, "Mechanical properties of calotropis procera/agave fiber

hybrid reinforced polyester composites," *International Journal of Printing, Packaging & Allied Sciences*, vol. 4, no. 5, pp. 3669–3673, 2017.

[25] C. Kandeepan, K. Raja, and P. Ganeshan, "Investigation on the mechanical properties of madar fiber reinforced in polymer matrix composites," *International Conference on Current Research in Engineering Science and Technology*, vol. 4, pp. 110–116, 2016.

[26] B. Ashok Kumar, K. Lingadurai, K. Raja, P. Ganeshan, and S. Vairam, "Prediction effect of fiber content on mechanical properties of banana and madar fiber hybrid polyester composites," *Advances in Natural and Applied Sciences*, vol. 10, no. 7, pp. 180–183, 2016.

[27] P. Ganeshan, K. Raja, K. Lingadurai, and M. Kaliappan, "Analysis of an automobile drive shaft with various composite materials," *International Journal of Applied Engineering Research*, vol. 10, no. 50, pp. 558–594, 2015.

[28] P. Ganeshan, K. Raja, K. Lingadurai, and M. Kaliappan, "Finite element analysis of alternate composite material for an automobile drive shaft," *International Journal of Applied Engineering Research*, vol. 10, no. 49, pp. 447–452, 2015.

[29] K. Yoganandam, K. Raja, and K. Lingadurai, "Mechanical and micro structural characterization of Al6082-TiO," *Indian Journal of Science and Technology*, vol. 9, no. 41, pp. 1–4, 2016.

[30] K. Raja, V. S. Raman, R. Parthasarathi, K. Ranjitkumar, and V. Mohanavel, "Performance analysis of dee-biodiesel blends in diesel engine," *International Journal of Ambient Energy*, 2019.

[31] V. S. Chandrasekar and K. Raja, "Material selection for automobile torsion bar using fuzzy topsis tool," *International Journal of Advances in Engineering & Technology*, vol. 7, no. 2, pp. 343–349, 2016.

[32] B. Babu, K. Raja, S. Dharmalingam, S. Udhayaraj, and V. Vairamani, "Electrochemical micro machining on hybrid metal matrix composites," *International Journal of ChemTech Research*, vol. 8, no. 2, pp. 508–518, 2015.

[33] M. Manikandan, K. Raja, and V. S. Chandrasekar, "Experimental investigation on torsion bar suspension system using e- glass fibre reinforced composite material," *International Journal of Renewable Energy Technology*, vol. 3, no. 11, pp. 2319–2322, 2014.

[34] G. Maruthupandian, R. Saravanan, S. Suresh Kumar, and B. G. Sivakumar, "A study on bamboo reinforced concrete slabs," *Journal of Chemical and Pharmaceutical Sciences*, vol. 9, no. 2, pp. 978–980, 2016.

[35] M. Rajeshwaran, K. Raja, and P. Velmurugan, "Duraimurugan alias saravanan "optimization of soxhlet extraction of prosopis julifera using response surface methodology"," *International Journal of Applied Engineering Research*, vol. 10, no. 49, pp. 552–557, 2015.

[36] G.-Wu Yang, L. Yang, S.-Ne Xiao, S.-L. Jiang, and W. Ma, "Competitive failure of loosening and fatigue of bolts under composite excitation," *Shock and Vibration*, vol. 2021, Article ID 1441122, 13 pages, 2021.